

# Preparation of Chitosan-Coated Nanoliposomes for Improving the Mucoadhesive Property of Curcumin Using the Ethanol Injection Method

Gye Hwa Shin,<sup>†,§</sup> Seoung Kyun Chung,<sup>†,§</sup> Jun Tae Kim,<sup>‡</sup> Hee Joung Joung,<sup>†</sup> and Hyun Jin Park<sup>\*,†</sup>

<sup>†</sup>College of Life Sciences & Biotechnology, Korea University, Anam-dong, Seongbuk-gu, Seoul 136-701, Korea

<sup>‡</sup>Department of Food Science and Technology, Keimyung University, Daegu 704-701, Korea

**ABSTRACT:** Chitosan-coated curcumin nanoliposomes (CS-Cur-NLs) were fabricated by the ethanol injection method (EIM), and their physicochemical properties were compared with the properties of those fabricated by the dry thin film method (DTFM). The mean size and zeta potential of CS-Cur-NLs gradually increased with CS concentration. The encapsulation efficiency of Cur-NLs prepared by EIM was 54.70%, which was significantly improved compared to that (42.60%) of Cur-NLs prepared by DTFM. Further improvement of encapsulation efficiency was attained (up to 64.93%) by EIM with 0.1% CS coating. The mucoadhesive property of Cur-NLs improved from 33.60 to 56.47% with CS coating. The results indicate that the encapsulated curcumin will show prolonged adsorption in the gastrointestinal tract because of higher mucoadhesion. Thus, EIM can be considered to be effective for food-grade delivery carriers with higher encapsulation efficiency and absence of harmful solvents. EIM-generated CS-Cur-NLs showed higher bioavailability, with enhanced high mucoadhesive property, storage stability, and encapsulation efficiency.

**KEYWORDS:** nanoliposomes, curcumin, chitosan, ethanol injection method, mucoadhesive property

## ■ INTRODUCTION

Curcumin, a natural polyphenolic nutraceutical, has been widely used as a traditional medicine in many Asian countries, since it was reported that curcumin has antioxidant, anti-inflammatory, antimicrobial, and anticancer features, as well as wound healing characteristics.<sup>1–5</sup> Although curcumin has numerous advantages, the therapeutic application of curcumin is limited because of its poor solubility and low bioavailability. In order to improve its bioavailability, water solubility, and functionality, many researchers have studied the fabrication of various micro- to nanosized carrier systems, such as polymeric nanoparticles, solid lipid nanoparticles, emulsions, hydrogels, biodegradable microspheres, and liposomes.<sup>6–11</sup>

Liposomes have been extensively studied for transporting drugs and functional foods with poor water solubility through the improvement of their stability, clinical efficacy, and bioavailability.<sup>12–15</sup> As spherical vesicles composed of bilayer membranes, liposomes can carry both hydrophilic and hydrophobic components by encapsulation in the water phase and intercalating into the hydrophobic domains, respectively. Even hydrophobic components can be formed in a stable state in an aqueous environment by high dispersion in a liposome system. In addition, the components entrapped in liposomes can effectively penetrate and overcome biological barriers to cellular and tissue uptake because the liposome has a similar structure as the cell membrane.<sup>12</sup> Generally, lipophilic and/or water insoluble nutraceuticals such as curcumin show low bioavailability in an oral delivery system. In order to improve bioavailability and to overcome this limitation, many studies have been performed to prolong the gastrointestinal (GI) tract time by using a floating drug dosage system, modified shape system, and mucoadhesive system.<sup>16,17</sup> One of the most

extensively investigated systems for prolonging the residence time in the GI tract is the modification of mucoadhesive polymers on the delivery carriers, resulting in the improvement of adsorption through the mucosa and release of the loaded cores in a sustained manner. Since mucin has negatively charged sialic acid groups, the positively charged polymer coating of the liposomes could be more effective in prolonging the retention time of core materials by improving the interaction with the intestinal wall mucus and avoiding rapid clearance from the delivery target.<sup>18</sup> The mucoadhesive property of delivery carriers is a complex phenomenon, and the mucoadhesion can occur by electronic interaction, wetting, adsorption, diffusion, and mechanical interaction between mucoadhesive polymers and a biological mucosal surface.<sup>19</sup> In most cases, the mucoadhesive property of delivery carriers can be improved by delaying the intestinal transit time and increasing the adsorption of core materials.<sup>20</sup>

Among various biopolymers, chitosan (CS) has been widely studied as a mucoadhesive material that enhances the penetration of macromolecules across the intestinal and nasal barriers.<sup>21</sup> CS is predominantly composed of  $\beta$ -(1,4)-linked D-glucosamine units and is obtained by deacetylation of chitin, which is the primary component of the cell walls of crustaceans, fungi, and insects.<sup>22</sup> CS is attractive as a coating polymer for food grade liposomes because of its nontoxic, biocompatible, and biodegradable characteristics, as well as unique cationic feature in the aqueous condition.<sup>23,24</sup> CS coating generates the

**Received:** August 9, 2013

**Revised:** October 25, 2013

**Accepted:** October 31, 2013

**Published:** October 31, 2013

positive charge on mucoadhesive liposomes by forming electrostatic interactions between positively charged CS and negatively charged diacetyl phosphates on the surfaces of the liposomes.<sup>25</sup>

To date, liposomal curcumin has been mainly prepared by the dry thin film method (DTFM), which was the initial method used to prepare liposomes.<sup>26</sup> Although it is an easy and widely used method, DTFM has some drawbacks, in terms of suitability for many applications and the requirement that excludes organic solvents, such as chloroform and hexane, especially in food grade products. When liposomes are applied to food grade products, the use of organic solvents should be avoided in their preparation as much as possible. It was reported that the ethanol injection method (EIM) has some limitations in poor encapsulation efficiency (below 40%) in hydrophilic substances. However, EIM is more desirable than DTFM for hydrophobic components, such as curcumin, to produce food-grade liposomes because it is free from harmful chemicals and can yield a more homogeneous population.<sup>27</sup> On the basis of our literature review, there has been no research on the curcumin nanoliposomes (Cur-NLs) using EIM.

In the present study, CS-coated curcumin nanoliposomes (CS-Cur-NLs) were synthesized using both EIM and DTFM, and their physicochemical properties were compared. The effects of CS coating on the particle size, polydispersity index (PDI), zeta potential, encapsulation efficiency, and mucin adsorption of Cur-NLs and CS-Cur-NLs were investigated.

## MATERIALS AND METHODS

**Chemicals.** CS (molecular weight, 30 000; degree of deacetylation, 88%) was obtained from BioTech Co. Ltd. (Mokpo-si, Jeollanam-do, Korea). 1- $\alpha$ -Phosphatidylcholine (EPC, from dried egg yolk,  $\geq 60\%$  TLC), cholesterol ( $\geq 95\%$ ), dichloromethane, mucin (extracted from porcine stomach, type III), and Bradford reagent were purchased from Sigma-Aldrich (St. Louis, MO, USA). Curcumin (mixture of demethoxy curcumin and bisdemethoxy curcumin,  $\geq 98\%$ ) was purchased from Acros (Belgium, USA). Analytical grade ethanol and acetone were purchased from Duksan (Anshan-si, Gyeonggi-do, Korea).

**Preparation of Curcumin Nanoliposomes (Cur-NLs) and CS-Coated Curcumin Nanoliposomes (CS-Cur-NLs) by the Ethanol Injection Method (EIM).** Cur-NLs were formed by utilizing the amphiphilic property of EPC as a surfactant. EPC and cholesterol (as a shape stabilizer) were dissolved in ethanol containing curcumin. The molar ratio of EPC and cholesterol was 2:1. Curcumin and EPC were mixed in a ratio of 1:10 (w/w). The resulting solution was dropped into aqueous solution (Millipore Milli-Q system) and stirred for several hours until NLs formed spontaneously after further evaporation of the residual ethanol. The initial liposomes formed by self-assembly with mild stirring. These were reduced in size by ultrasonic homogenization using a model VCX 750 apparatus (Sonics & Materials, Newtown, CT, USA) for 15 min. The supernatant containing the Cur-NLs was separated from the insoluble excess curcumin in the pellet by centrifugation at 190g for 10 min. Cur-NLs were coated with various concentrations of CS solution. The CS solution (0.1, 0.2, 0.3, 0.4, or 0.5%, w/v) was prepared by dissolving CS in distilled water containing 0.1% (w/v) acetic acid. In order to remove the impurities, CS solution was filtered using a 0.45  $\mu\text{m}$  syringe filter (Minisart, Germany). The prepared CS solution was added dropwise to the Cur-NL solution. The CS-Cur-NLs were filtered using a 0.45  $\mu\text{m}$  membrane filter to characterize their physicochemical properties.

**Preparation of Cur-NLs and CS-Cur-NLs by the Dry Thin Film Method (DTFM).** To compare the characteristics of Cur-NLs obtained by EIM, Cur-NLs obtained by DTFM were also prepared. The same amount of curcumin used in EIM was first added to the mixture of EPC and cholesterol in a ratio of 2:1. The curcumin-

containing mixture was dissolved in dichloromethane, and a thin film of Cur-NLs was formed using a rotary evaporator. The resulting thin film was hydrated with Milli-Q water for 1 h and then treated with an ultrasonic homogenizer for 15 min. The final Cur-NL solution was filtered using a 0.45  $\mu\text{m}$  membrane filter to characterize its physicochemical properties. For preparation of CS-Cur-NLs by DTFM, a chitosan coating process was performed as mentioned in the previous section.

**Fourier Transform Infrared (FT-IR).** Structural characterization of CS-NLs was performed by Fourier transform infrared (FT-IR) using a model V430 apparatus (Jasco, Tokyo, Japan) at 20 °C. The FT-IR spectra of CS, CS-NLs, and NLs without the core material (curcumin) and cholesterol were obtained to verify the interactions between phosphatidylcholine and CS. The NL samples were mixed with potassium bromide (KBr) at a ratio of 1:10, and prepared as a 1 mm semitransparent pellet by compression under a force of 5 tons in a hydraulic press. Each spectrum was obtained from the average of 64 scans at a resolution of 2  $\text{cm}^{-1}$  in the wavelength range 4000–800  $\text{cm}^{-1}$ .

**Measurements of the Mean Particle Size, PDI, and Zeta Potential.** The mean size, PDI, and zeta potential of Cur-NLs and CS-Cur-NLs were measured using dynamic light scattering with a nano-ZS nanosize analyzer (Malvern, Worcestershire, U.K.). Three milliliters of Cur-NL dispersion was added to polystyrene latex cells, and the mean particle size, PDI, and zeta potential were measured at 25 °C with a detector angle of 90°, wavelength of 633 nm, refractive index of 1.33, and real refractive index of 1.59. Each sample was measured at least three times, and the average values were used.

**Storage Stability.** For testing the stability of Cur-NLs, the changes in mean size and PDI values were investigated over the storage periods. Cur-NLs and 0.1% CS-Cur-NLs prepared by DTFM and EIM were kept in an incubator at 25 and 4 °C. The mean particle size and PDI were measured using the same testing procedure explained in section 2.5 over the storage periods of 1, 3, 5, 7, 15, and 40 days.

**Encapsulation Efficiency.** The sample was centrifuged at 190g in a Hitachi centrifuge for 10 min, and the supernatant containing Cur-NLs was separated from the pellet. The pellet contained unloaded curcumin. The supernatant was recentrifuged two more times. Each time the pellet was dissolved in methanol, three fractions were pooled and quantified. After this step, the centrifuged supernatant sample was recentrifuged at 34 300g for 1 h to separate the curcumin in the pellet. The quantity of curcumin in the supernatant was determined using UV spectrum at 425 nm. The encapsulation efficiency (%) of curcumin was calculated using the equation below:

$$\text{Encapsulation efficiency (\%)} = [(C_t - C_f)/C_t] \times 100$$

where  $C_t$  is the total amount of curcumin used and  $C_f$  is the free curcumin in the supernatant.

**Mucin Adsorption Studies.** In order to evaluate the mucoadhesive properties of Cur-NLs and CS-Cur-NLs, a mucin adsorption test was carried by a slightly modified method<sup>23</sup> and the amount of free mucin was calculated by using the Bradford colorimetric method.<sup>28</sup> Briefly, 2 mL of mucin solution (1 mg/mL) was mixed with 2 mL of Cur-NLs or CS-Cur-NLs at 37 °C for 1 h. Then, the suspension was centrifuged at 10 600g at 4 °C for 30 min to separate the free mucin (supernatant) and adsorbed mucin (pellet). Bradford reagent diluted 5-fold was added to the supernatant and incubated in a 37 °C shaking incubator, shaking at 185 rpm for 10 min. The quantity of mucin in the supernatant was determined by measuring the absorbance at 595 nm. To make a standard curve, the absorbances of pure mucin solutions of 31.25, 62.5, 125, 250, 500, and 1000  $\mu\text{g/mL}$  were also measured. Mucin adsorption (%) was calculated using the equation below:

$$\text{Mucin adsorption (\%)} = [(C_t - C_f)/C_t] \times 100$$

where  $C_t$  is the total amount of mucin used and  $C_f$  is the free mucin in the supernatant.

**Transmission Electron Microscopy (TEM).** To prepare TEM samples, CS-NLs were dropped onto the carbon-coated grids for 1

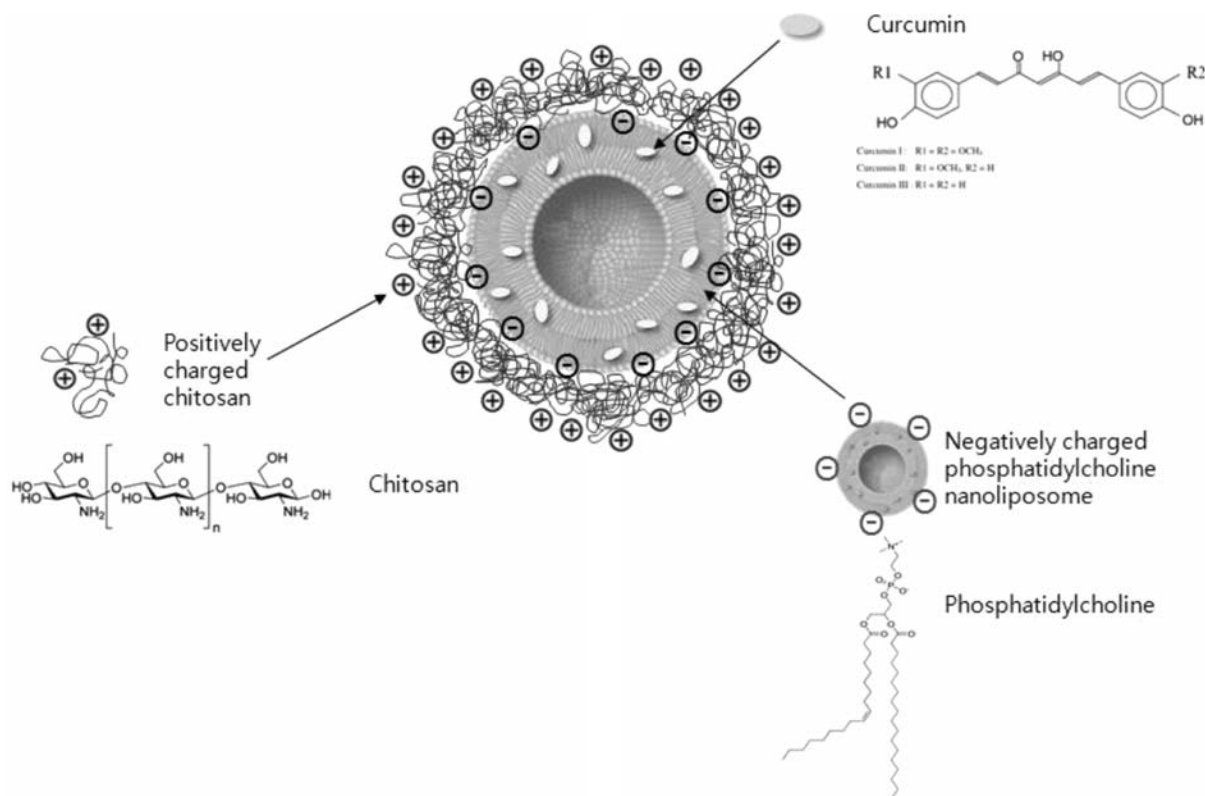


**Figure 1.** Schematic representation of chitosan-coated curcumin nanoliposome (CS-Cur-NLs).

min, and the excess was removed with filter paper. This step was repeated three times. Finally, the grids were stained with uranyl acetate (UA) or phosphotungstate (PTA) for 3 min and dried overnight and imaged using a TECNAI G2 F30 TEM (Philips-FEI, Eindhoven, Holland).

**Statistical Analysis.** Particle size and zeta potential of NLs were statistically analyzed using analysis of variance (ANOVA). Statistical Package for the Social Science (SPSS, Version 20.0, SPSS Inc., Chicago, IL, USA) was used for this analysis. Duncan's multiple range tests were used to determine the statistical significance among the means at 95% significant level.

## RESULTS AND DISCUSSION

**Characterization of CS-Cur-NLs.** Cur-NLs were fabricated by DTFM and EIM. A CS coating was applied to improve the mucoadhesive property of Cur-NLs. On the basis of the findings from our previous study, we chose a 2:1 ratio of EPC to cholesterol to obtain uniform and stable NLs. EPC acts as a structural material to form the liposome membrane, while cholesterol acts as a stabilizer to make liposomes more stable under aqueous conditions. Figure 1 shows the schematics of the CS-Cur-NLs formed by the ionic interaction between EPC and CS. A liposome is a spherical vesicle consisting of lipid bilayers and can encapsulate hydrophilic core materials. Hydrophobic cores, however, also can be encapsulated between lipid bilayers formed by double carbon chains of surfactants. The phospholipids can form ionized phosphate ( $\text{PO}_4^{3-}$ ) groups in aqueous conditions and entrap the hydrophobic curcumin in the lipid bilayers. This was verified by a fluorescence intensity test of curcumin and liposome bilayers.<sup>29</sup> CS-Cur-NLs were formed by colloidal forces such as van der Waals, hydrogen bonding, and electrostatic interactions. The most vital interaction in CS-Cur-NLs may be the electrostatic interactions between the positive charges of CS amine ( $\text{NH}_3^+$ ) groups and

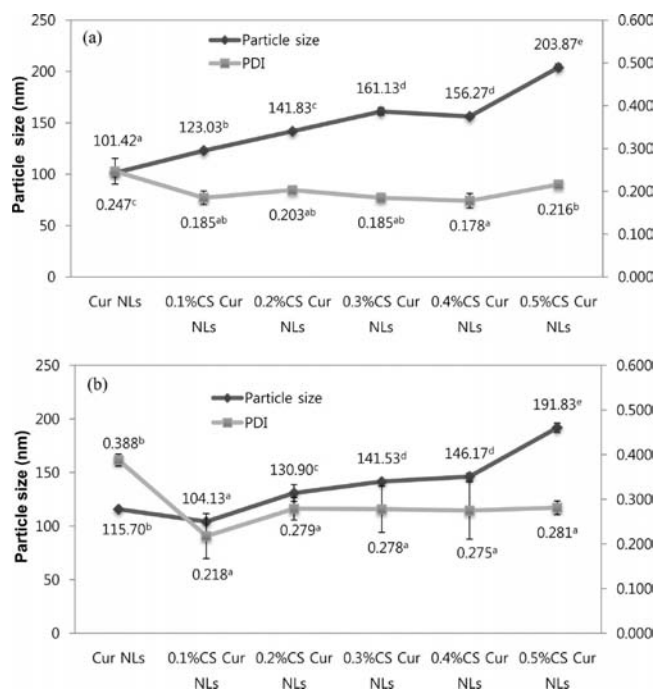


**Figure 2.** The effect of chitosan concentration on the mean size and PDI value of CS-Cur-NLs by (a) EIM and (b) DTFM. Different superscript letters indicate a significant difference at  $P < 0.05$  by Duncan's multiple range test.

the negative charges of liposome phosphate ( $\text{PO}_4^{3-}$ ) groups. CS-Cur-NLs had positive surface charges because of the CS coating. The main reason of the CS coating on the nanoliposome surface is to apply the intranasal delivery system

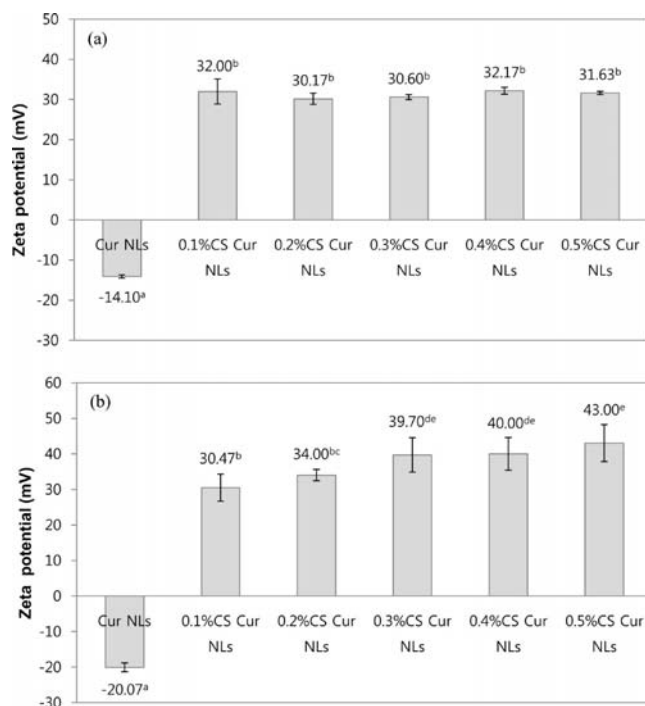


**Figure 3.** The effect of chitosan concentration on the zeta potential of CS-Cur-NLs by (a) EIM and (b) DTFM. Different superscript letters indicate a significant difference at  $P < 0.05$  by Duncan's multiple range test.

to improve bioavailability of curcumin. It has been reported that CS-coated nanoparticles improved the biocompatibility and mucoadhesiveness of drug loaded vesicles.<sup>23</sup>

**Effect of CS Coating on Size, PDI, and Zeta Potential of Curcumin NLs.** The effect of CS coating on curcumin NLs (Cur-NLs) was investigated by measuring the mean particle size, PDI, and zeta potential. Figure 2 shows the mean particle sizes and PDI values of Cur-NLs and CS-Cur-NLs prepared by EIM and DTFM. The mean particle sizes and PDI values of Cur-NLs were 101.42 nm and 0.247 for EIM and 115.70 nm

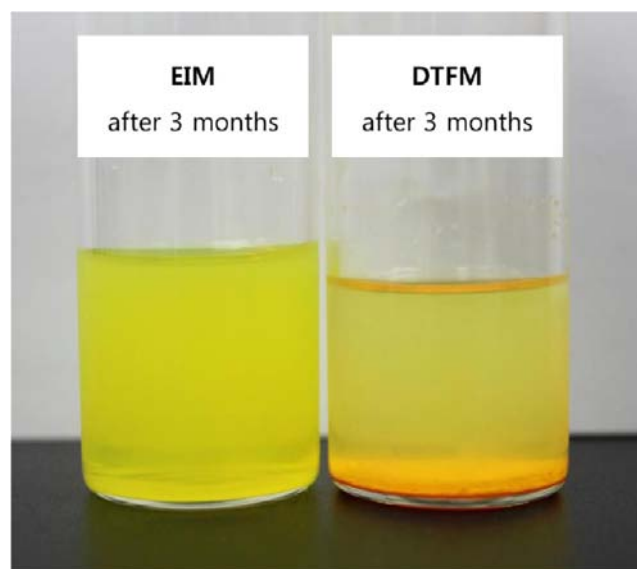


**Figure 4.** Comparison of the visual appearance of Cur-NLs prepared by (a) EIM and (b) DTFM after 3 months of storage at 4 °C.

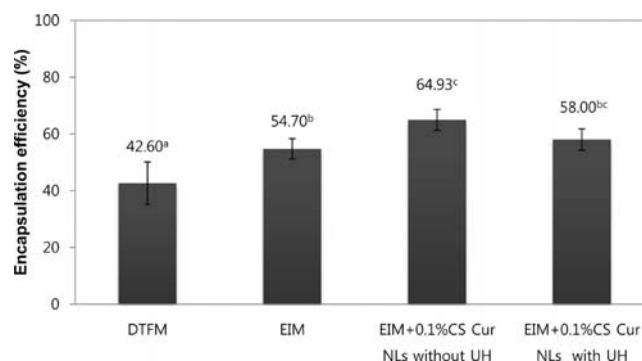


**Figure 5.** Encapsulation efficiency of curcumin by DTFM, EIM, or EIM + 0.1% CS with and without ultrasonic homogenization. Different superscript letters indicate a significant difference at  $P < 0.05$  by Duncan's multiple range test.

**Table 1.** The Stability of Cur-NLs and 0.1% CS-Cur-NLs by DTFM and EIM (a) at 25 °C and (b) at 4 °C<sup>a</sup>

	(a)					
	DTFM_25 °C		EIM_25 °C		EIM_0.1%CS_25 °C	
	size (nm)	PDI	size (nm)	PDI	size (nm)	PDI
1 day	114.83 ± 1.01 ab	0.391 ± 0.004 c	81.54 ± 0.27 abc	0.269 ± 0.022 b	138.97 ± 1.58 ab	0.208 ± 0.018 bc
3 days	116.53 ± 2.02 b	0.395 ± 0.008 c	85.88 ± 1.18 c	0.303 ± 0.013 c	141.47 ± 2.47 bc	0.213 ± 0.005 c
5 days	114.80 ± 2.23 ab	0.395 ± 0.005 c	90.91 ± 5.10 d	0.342 ± 0.025 d	138.13 ± 2.19 ab	0.202 ± 0.006 ab
7 days	116.67 ± 3.07 b	0.406 ± 0.016 c	83.35 ± 0.74 bc	0.245 ± 0.018 b	143.23 ± 2.82 c	0.205 ± 0.031 bc
15 days	112.70 ± 0.87 a	0.347 ± 0.011 b	78.56 ± 0.85 a	0.190 ± 0.013 a	135.57 ± 1.50 a	0.175 ± 0.007 a
40 days	114.30 ± 0.61 ab	0.282 ± 0.029 a	79.13 ± 0.56 ab	0.183 ± 0.004 a	136.70 ± 1.37 a	0.181 ± 0.009 ab
	(b)					
	DTFM_4 °C		EIM_4 °C		EIM_0.1%CS_4 °C	
	size (nm)	PDI	size (nm)	PDI	size (nm)	PDI
1 day	114.97 ± 2.31 b	0.366 ± 0.048 b	81.38 ± 0.86 b	0.272 ± 0.004 b	132.97 ± 1.61 bc	0.221 ± 0.018 ab
3 days	114.28 ± 2.95 b	0.379 ± 0.004 b	85.56 ± 0.59 cd	0.335 ± 0.035 c	134.67 ± 1.25 c	0.213 ± 0.013 ab
5 days	116.60 ± 1.83 b	0.399 ± 0.019 b	87.92 ± 3.82 d	0.306 ± 0.031 bc	138.37 ± 1.25 d	0.234 ± 0.014 b
7 days	142.10 ± 3.82 c	0.588 ± 0.021 c	84.36 ± 0.63 c	0.281 ± 0.008 b	132.40 ± 1.35 b	0.225 ± 0.013 ab
15 days	112.37 ± 1.65 b	0.374 ± 0.008 b	78.59 ± 0.49 ab	0.182 ± 0.013 a	133.93 ± 0.50 bc	0.237 ± 0.017 b
40 days	99.75 ± 1.31 a	0.264 ± 0.005 a	77.09 ± 0.46 a	0.194 ± 0.007 a	128.03 ± 0.25 a	0.208 ± 0.011 a

<sup>a</sup>Different online letters indicate a significant difference at  $P < 0.05$  by Duncan's multiple range test.

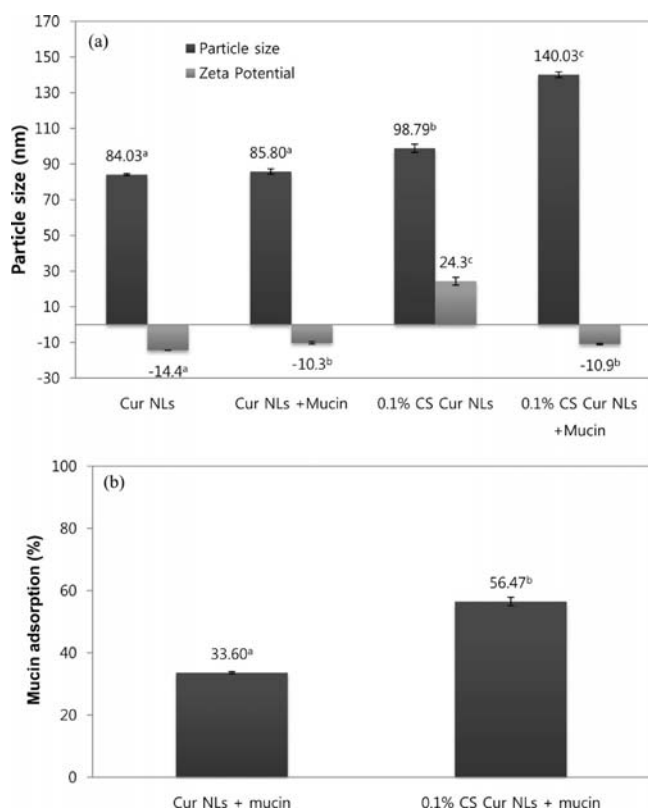


**Figure 6.** Effect of chitosan coating on (a) the mean size and zeta potential of Cur-NLs before and after mucin association and 0.1% CS coating and (b) mucin adsorption of Cur-NLs and CS-Cur-NLs.

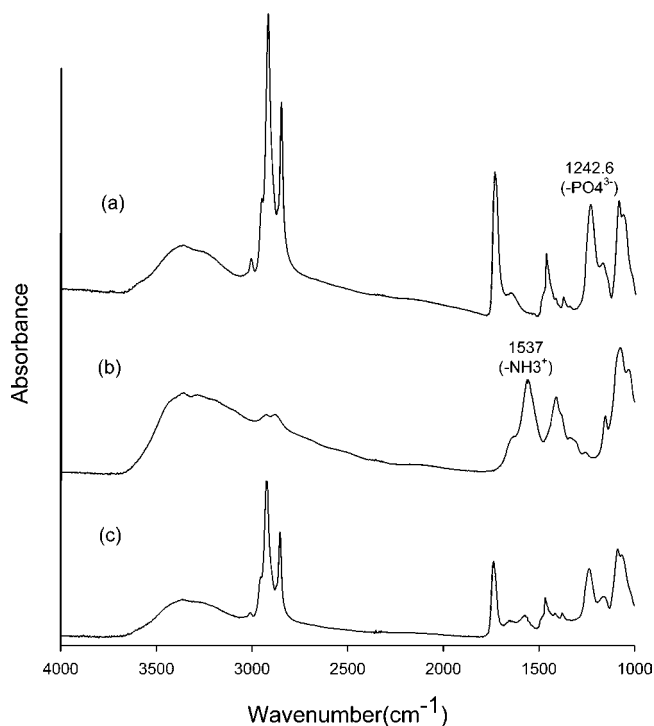


**Figure 7.** FT-IR spectra of (a) phosphatidylcholine nanoliposomes (PC-NLs), (b) 0.1% CS solution, and (c) 0.1% CS-NLs.

and 0.388 for DTFM, respectively. The particle size significantly ( $P < 0.05$ ) increased with CS concentration with both EIM and DTFM, whereas PDI values significantly ( $P <$

0.05) decreased after CS coating but the decrease was not statistically significant ( $P > 0.05$ ) with CS concentration, as shown in Figure 2. The particle sizes of CS-Cur-NLs obtained by EIM were slightly larger (about 10–15%) than those obtained by DTFM in the entire CS concentration range. The maximum size of 203.87 nm was obtained in 0.5% (w/v) CS-Cur-NLs by EIM. As a heterogeneity index, a higher PDI value indicates that the dispersion is more heterogeneous, whereas a lower PDI value indicates that the dispersion is more homogeneous. PDI values of CS-Cur-NLs obtained by DTFM were about 20–55% higher than those obtained by EIM. This result suggests that homogeneous CS-Cur-NLs were obtained by EIM compared to those obtained by DTFM.

Figure 3 shows the zeta potential of CS-Cur-NLs obtained by EIM and DTFM. Zeta potentials of Cur-NLs by EIM and DTFM were  $-14.10$  and  $-20.07$  mV, respectively. As expected, Cur-NLs were negatively charged because of the diacetyl phosphates on the surfaces of the liposomes. However, CS coating changed the surface charge to positive because of the positively charged amine groups of CS. With various CS concentrations, zeta potentials of CS-Cur-NLs ranged from  $+30.17$  to  $+32.17$  mV for EIM and from  $+30.47$  to  $+43.00$  mV for DTFM. It was reported that liposome concentration could be diluted with additional ethanol during the EIM process.<sup>27</sup> Consequentially, a higher zeta potential of CS-Cur-NLs by DTFM could be obtained due to the higher liposome concentration than those by EIM. It is possible that the CS coating could make NLs more stable vesicles and more effective for homogeneous particle distribution. In addition, the surface of CS-coated NLs showed hydrophilic properties. The hydrophilic and positively charged surface properties enhanced adsorption by the epithelial cells. The most important characteristic of CS-coated NLs is the improved target effect on tumor cells, as well as on gene expression.<sup>30,31</sup>

**Stability of Curcumin NLs.** The stability of Cur-NLs and CS-Cur-NLs was evaluated by measuring the change in their mean size and PDI value over time. Cur-NL samples were stored at 4 and 25 °C for up to 40 days, and the particle size and PDI were measured at 1, 3, 5, 7, 15, and 40 days. The mean size and PDI values of Cur-NLs and 0.1% CS-Cur-NLs by DTFM and EIM are summarized in Table 1. The mean size of Cur-NLs by DTFM was around 115 nm and did not significantly change ( $P > 0.05$ ) at 25 °C until 40 days, whereas the mean size at 4 °C did not change during storage, except at 7 and 40 days. Bigger particle sizes of Cur-NLs by DTFM at 7 days may be mainly ascribed to swelling of Cur-NLs over time. The particle size of Cur-NLs by DTFM was decreased after 15 and 40 days. This may be mainly due to the release of curcumin from nanoliposomes. On the other hand, the mean size of Cur-NLs by EIM was significantly ( $P < 0.05$ ) increased both at 25 and 4 °C until 5 days and decreased further during storage. CS coating also increased the mean particle size from around 80–90 to over 130 nm. However, the change in mean particle size of CS-Cur-NLs by EIM over the storage period showed the same trends as Cur-NLs obtained by EIM. Although there were some significant changes ( $P < 0.05$ ), the Cur-NLs prepared by EIM showed high stability at 25 and 4 °C until 40 days, and their stability was similar to that of Cur-NLs prepared by DTFM. However, the stability of Cur-NLs prepared by EIM and DTFM was totally different after 3 months of storage at 4 °C. Figure 4 shows a comparison of visual appearance of Cur-NLs prepared by (a) EIM and (b) DTFM after 3 months of storage at 4 °C. As shown in Figure 4a, Cur-NLs by EIM

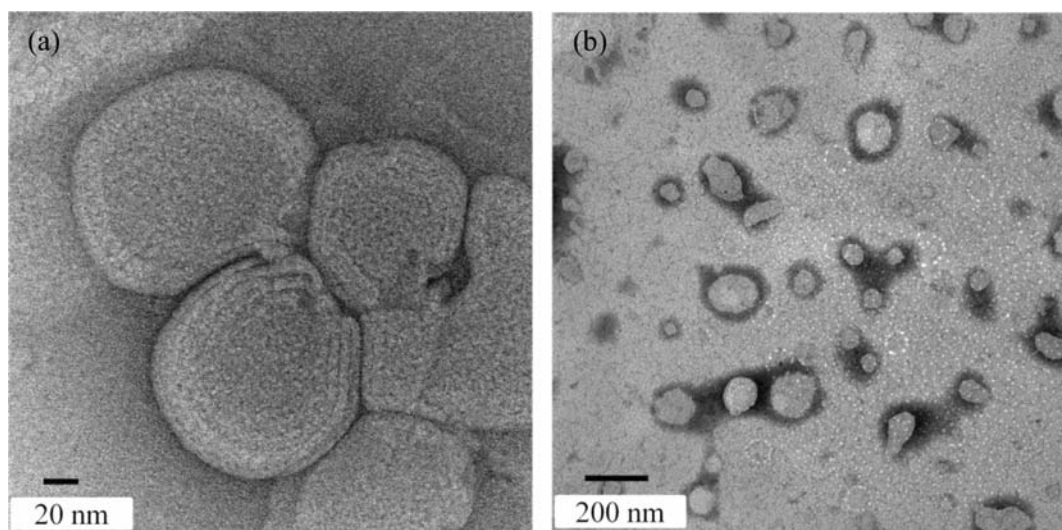


**Figure 8.** Transmission electron microscope images of CS-Cur-NLs with (a) a scale bar of 20 nm and (b) a scale bar of 200 nm.

showed still good dispersion and any precipitation or sedimentation was not observed. Their mean size and PDI values were not significantly changed until 3 months of storage, and they were around 90 nm and less than 0.3, respectively. However, Cur-NLs by DTFM were not stable and serious sedimentation was observed, as shown in Figure 4b. Although Cur-NLs by EIM and DTFM showed similar stability within 40 days, Cur-NLs by DTFM were precipitated on long-term storage.

**Encapsulation Efficiency of Cur-NLs.** The curcumin encapsulation efficiency in Cur-NLs and CS-Cur-NLs was determined by measuring the amount of free curcumin. The encapsulation efficiency of core materials in the delivery system is primarily dependent on the physicochemical characteristics of core materials, such as the hydrophilicity/hydrophobicity and solubility.<sup>32</sup> Typically, curcumin has poor solubility (<1 mg/mL in ethanol and <0.011 mg/mL in water), and its solubility is very sensitive to pH, rarely solubilizing in acidic solutions.<sup>33</sup> In addition, the encapsulation efficiency depends on the size and components of liposomes, including phospholipids and stabilizer (cholesterol). Figure 5 shows the encapsulation efficiency of Cur-NLs obtained by DTFM and EIM. The encapsulation efficiency of Cur-NLs prepared by EIM was 54.70%, which was about 28% higher than that of Cur-NLs prepared by DTFM. In this case, other factors such as the mixing ratio, amount, and type of cholesterol, phospholipid, and core material were kept constant. It has been reported that the encapsulation efficiency of hydrophilic core liposomes by EIM was generally low because of high volume usage.<sup>27</sup> In the case of hydrophobic curcumin, however, the encapsulation efficiency of EIM was improved compared to DTFM, and the values were statistically significant ( $P < 0.05$ ), as shown in Figure 5. CS coating also significantly ( $P < 0.05$ ) improved the encapsulation efficiency of curcumin from 54.70 to 64.93%, which is about 19% improvement. Further treatment by ultrasonic homogenization decreased the encapsulation efficiency to 58.00%. Although it may make CS-Cur-NLs homogeneous and improve their stability, mechanical power can negatively affect encapsulation efficiency.<sup>12</sup>

**Mucoadhesion Studies of Cur-NLs.** Mucus is the first barrier for nutrients, which interact with it and diffuse through it. As a large and extracellular glycoprotein, mucin is one of the

major components of mucus.<sup>34</sup> Figure 6a shows the mean size and zeta potential of Cur-NLs and CS-Cur-NLs with and without mucin association. As we explained in the previous section, the particle size of Cur-NLs was increased by CS coating. By mucin association, the particle size of CS-Cur-NLs increased from 98.79 to 140.03 nm, whereas the particle size of Cur-NLs was not significantly different ( $P > 0.05$ ). The zeta potential of Cur-NLs changed slightly, from  $-15.3$  to  $-10.3$  mV, whereas the zeta potential of CS-Cur-NLs changed greatly from  $+24.3$  to  $-10.9$  mV, as shown in Figure 6a. The changes in surface charge may result from interactions between negatively charged mucin and positively charged CS-Cur-NLs. The interaction between CS-Cur-NLs and mucin is mainly due to the electrostatic interaction between the amine group ( $\text{NH}_3^+$ ) of CS and the carboxylate ( $\text{COO}^-$ ) or sulfonate ( $\text{SO}_3^-$ ) group of mucin. The mucoadhesive properties of NLs were characterized by measuring their mucin adsorption. Mucin adsorption by Cur-NLs and CS-Cur-NLs was 33.60 and 56.47%, respectively, as shown in Figure 6b. Mucin adsorption of Cur-NLs could be improved by about 68% after CS coating. Mucin adsorption of Cur-NLs by DTFM could also be improved by chitosan coating because mucin adsorption is significantly depending on the surface characteristic. Since mucin proteins secreted from epithelial cells have negative charges, they can have more electrostatic interactions with positively charged CS. Our results suggest that CS-Cur-NLs stay at the target site longer than the Cur-NLs. On the other hand, the mucin adsorption of Cur-NLs was around 33.6%. This may be because curcumin molecules have several  $-\text{OH}$  groups and  $-\text{O}$  moieties, and thus, they could interact with mucin by hydrogen bonding.<sup>35</sup>

**FT-IR Analysis of CS-NLs.** FT-IR analysis was used to verify the interactions between CS and phosphatidylcholine on the NLs. Figure 7a is the spectrum of phosphatidylcholine NLs (PC-NLs). The peaks between  $1150$  and  $1400\text{ cm}^{-1}$  and at  $1465\text{ cm}^{-1}$  were assigned  $\text{CH}_2$ -wagging progression and  $\text{CH}_2$ -scissoring vibrations, which are considered particularly useful. The former is used as a measure of the degree of lipid acyl chain order, whereas the latter is regarded as an indication of chain packing effects. Two major peaks at  $1242$  and  $1742\text{ cm}^{-1}$  were assigned to antisymmetric  $\text{PO}_2^-$  stretching and  $\text{C}=\text{O}$  stretching, respectively. For native CS, two peaks at  $1662$  and

1556 cm<sup>-1</sup> were assigned to the carbonyl (C=O) stretching (amide I) and N—H bending vibration (amide II), respectively,<sup>36–38</sup> as shown in Figure 7b. The FT-IR spectrum of CS-NLs was the combination of PC-NLs and CS, as shown in Figure 7c. The FT-IR result supported that CS coated the PC-NLs well.

**Liposome Morphology.** The surface morphology of CS-Cur-NLs was characterized by transmission electron microscopy (TEM). Figure 8 shows the TEM images of CS-Cur-NLs at different locations. The morphology of CS-Cur-NLs was almost spherical, and the particle size ranged from 80 to 120 nm. CS-Cur-NLs had a contrasting dark band surrounding a liposome vesicle, as shown in Figure 8b. The interaction of CS with the surface of NLs was well visualized.

## AUTHOR INFORMATION

### Corresponding Author

\*Phone: 82-2-3290-4149. Fax: 82-2-953-5892. E-mail: hjpark@korea.ac.kr.

### Author Contributions

†These authors contributed equally to this work.

### Funding

This research was supported by a grant (13162MFDS777) from Ministry of Food and Drug Safety in 2013 and by the International Research & Development Program of the National Research Foundation of Korea (NRF) funded by the Ministry of Education, Science and Technology (MEST) of Korea (Grant No. 2012K1A3A1A20031356)

### Notes

The authors declare no competing financial interest.

## REFERENCES

- (1) Biswas, T. K.; Mukherjee, B. Plant medicines of Indian origin for wound healing activity: a review. *Int. J. Lower Extrem. Wounds* **2003**, *2*, 25–39.
- (2) Kunnumakkara, A. B.; Anand, P.; Aggarwal, B. B. Curcumin inhibits proliferation, invasion, angiogenesis and metastasis of different cancers through interaction with multiple cell signaling proteins. *Cancer Lett.* **2008**, *269*, 199–225.
- (3) Lantz, R. C.; Chen, G. J.; Solyom, A. M.; Jolad, S. D.; Timmermann, B. N. The effect of turmeric extracts on inflammatory mediator production. *Phytomedicine* **2005**, *12*, 445–452.
- (4) Pulla Reddy, A. Ch.; Lokesh, B. R. Studies on spice principles as antioxidants in the inhibition of lipid peroxidation of rat liver microsomes. *Mol. Cell. Biochem.* **1992**, *111*, 117–124.
- (5) Bhawana.; Basniwal, R. K.; Buttar, H. S.; Jain, V. K.; Jain, N. Curcumin nanoparticles: preparation, characterization, and antimicrobial study. *J. Agric. Food Chem.* **2011**, *59*, 2056–2061.
- (6) Xiao, Y.; Chen, X.; Yang, L.; Zhu, X.; Zou, L.; Meng, F.; Ping, Q. Preparation and oral bioavailability study of curcuminoid-loaded microemulsion. *J. Agric. Food Chem.* **2013**, *61*, 3654–3660.
- (7) Xie, X.; Tao, Q.; Zou, Y.; Zhang, F.; Guo, M.; Wang, Y.; Wang, H.; Zhou, Q.; Yu, S. PLGA nanoparticles improve the oral bioavailability of curcumin in rats: characterizations and mechanisms. *J. Agric. Food Chem.* **2011**, *59*, 9280–9289.
- (8) Bisht, S.; Mizuma, M.; Feldmann, G.; Ottenhof, N. A.; Hong, S. M.; Pramanik, D.; Chenna, V.; Karikari, C.; Sharma, R.; Goggins, M. G.; Rudek, M. A.; Ravi, R.; Maitra, A.; Maitra, A. Systemic administration of polymeric nanoparticle-encapsulated curcumin (nanocur) blocks tumor growth and metastases in preclinical models of pancreatic cancer. *Mol. Cancer Ther.* **2010**, *9*, 2255–2264.
- (9) Takahashi, M.; Uechi, S.; Takara, K.; Asikin, Y.; Wada, K. Evaluation of an oral carrier system in rats: bioavailability and antioxidant properties of liposome encapsulated curcumin. *J. Agric. Food Chem.* **2009**, *57*, 9141–9146.
- (10) Pan, K.; Zhong, Q.; Baek, S. J. Enhanced dispersibility and bioactivity of curcumin by encapsulation in casein nanocapsules. *J. Agric. Food Chem.* **2013**, *61*, 6036–6043.
- (11) Helgason, T.; Awad, T. S.; Kristbergsson, K.; Decker, E. A.; McClements, D. J.; Weiss, J. Impact of surfactant properties on oxidative stability of  $\beta$ -carotene encapsulated within solid lipid nanoparticles. *J. Agric. Food Chem.* **2009**, *57*, 8033–8040.
- (12) Brandl, M. Liposomes as drug carriers: a technological approach. *Biotechnol. Annu. Rev.* **2001**, *7*, 59–85.
- (13) Lazar, A. N.; Mourtas, S.; Youssef, I.; Parizot, C.; Dauphin, A.; Delatour, B.; Antimisiaris, S. G.; Duyckaerts, C. Curcumin-conjugated nanoliposomes with high affinity for A $\beta$  deposits: possible applications to Alzheimer disease. *Nanomed. Nanotechnol. Biol. Med.* **2013**, *9*, 712–721.
- (14) Li, L.; Ahmed, B.; Mehta, K.; Kurzrock, R. Liposomal curcumin with and without oxaliplatin: effects on cell growth, apoptosis, and angiogenesis in colorectal cancer. *Mol. Cancer Ther.* **2007**, *6*, 1276–1282.
- (15) Saul, J. M.; Annapragada, A.; Natarajan, J. V.; Bellamkonda, R. V. Controlled targeting of liposomal doxorubicin via the folate receptor in vitro. *J. Controlled Release* **2003**, *92*, 49–67.
- (16) Choi, B. Y.; Park, H. J.; Hwang, S. J.; Park, J. B. Preparation of alginate beads for floating drug delivery system: effects of CO<sub>2</sub> gas-forming agents. *Int. J. Pharm.* **2002**, *239*, 81–91.
- (17) Chun, M. K.; Cho, C. S.; Choi, H. K. Mucoadhesive microspheres prepared by interpolymer complexation and solvent diffusion method. *Int. J. Pharm.* **2005**, *288*, 295–303.
- (18) Soane, R. J.; Frier, M.; Perkins, A. C.; Jones, N. S.; Davis, S. S.; Illum, L. Evaluation of the clearance characteristics of bioadhesive systems in humans. *Int. J. Pharm.* **1999**, *178*, 55–65.
- (19) Peppas, N. A.; Sahlin, J. J. Hydrogels as mucoadhesive and bioadhesive materials: a review. *Biomaterials* **1996**, *17*, 1553–1561.
- (20) Aspden, T. J.; Mason, J. D. T.; Jones, N. S.; Lowe, J.; Skaugrud, O.; Illum, L. Chitosan as a nasal delivery system: the effect of chitosan solutions on *in vitro* mucociliary transport rates in human turbinates and volunteers. *J. Pharm. Sci.* **1997**, *86*, 509–513.
- (21) Lee, J. W.; Park, J. H.; Robinson, J. R. Bioadhesive-Based Dosage Forms: The Next Generation. *J. Pharm. Sci.* **2000**, *89*, 850–866.
- (22) Muzzarelli, R. A. A.; Boudrant, J.; Meyer, D.; Manno, N.; DeMarchis, M.; Paoletti, M. G. Current views on fungal chitin/chitosan, human chitinases, food preservation, glucans, pectins and inulin: a tribute to Henri Braconnot, precursor of the carbohydrate polymers science, on the chitin bicentennial. *Carbohydr. Polym.* **87**, 995–1012.
- (23) Filipović-Grčić, J.; Škalko-Basnet, N.; Jalšenjak, I. Mucoadhesive chitosan-coated liposomes: characteristics and stability. *J. Microencapsulation* **2001**, *18*, 3–12.
- (24) Tozaki, H.; Odoriba, T.; Okada, N.; Fujita, T.; Terabe, A.; Suzuki, T.; Okabe, S.; Muranishi, S.; Yamamoto, A. Chitosan capsules for colon-specific drug delivery: enhanced localization of 5-aminosalicylic acid in the large intestine accelerates healing of TNBS-induced colitis in rats. *J. Controlled Release* **2002**, *82*, 51–61.
- (25) Takeuchi, H.; Yamamoto, H.; Niwa, T.; Hino, T.; Kawashima, Y. Mucoadhesion of polymer-coated liposomes to rat intestine *in vitro*. *Chem. Pharm. Bull.* **1994**, *42*, 1954–1956.
- (26) Bangham, A. D.; Standish, M. M.; Watkins, J. C. Diffusion of univalent ions across the lamellae of swollen phospholipids. *J. Mol. Biol.* **1965**, *13*, 238–252.
- (27) Pons, M.; Foradada, M.; Estelrich, J. Liposomes obtained by the ethanol injection method. *Int. J. Pharm.* **1993**, *95*, 51–56.
- (28) Bradford, M. M. A Rapid and Sensitive Method for the Quantitation of microgram quantities of protein utilizing the principle of protein-dye binding. *Anal. Biochem.* **1976**, *72*, 248–254.
- (29) Karewicz, A.; Bielska, D.; Gzyl-Malchera, B.; Kepczynska, M.; Lach, R.; Nowakowska, M. Interaction of curcumin with lipid monolayers and liposomal bilayers. *Colloids Surf., B* **2011**, *88*, 231–239.

- (30) Kim, J. H.; Kim, Y. S.; Park, K.; Lee, S.; Nam, H. Y.; Min, K. H.; Jo, H. G.; Park, J. H.; Choi, K.; Jeong, S. Y.; Park, R. W.; Kim, I. S.; Kim, K.; Kwon, I. C. Antitumor efficacy of cisplatin-loaded glycol chitosan nanoparticles in tumor-bearing mice. *J. Controlled Release* **2008**, *127*, 41–49.
- (31) Maitani, Y.; Igarashi, S.; Sato, M.; Hattori, Y. Cationic liposome (DC-Chol/DOPE=1:2) and a modified ethanol injection method to prepare liposomes, increased gene expression. *Int. J. Pharm.* **2007**, *342*, 33–39.
- (32) Karn, P. R.; Vanić, Z.; Pepić, I.; Škalko-Basnet, N. Mucoadhesive liposomal delivery systems: the choice of coating material. *Drug Dev. Ind. Pharm.* **2011**, *37*, 482–488.
- (33) Yallapu, M. M.; Jaggi, M.; Chauhan, S. C. Curcumin nanoformulations: a future nanomedicine for cancer. *Drug Discovery Today* **2012**, *17*, 71–80.
- (34) Bansil, R.; Turner, B. S. Mucin structure, aggregation, physiological functions and biomedical applications. *Curr. Opin. Colloid Interface Sci.* **2006**, *11*, 164–170.
- (35) Smart, J. D. The basics and underlying mechanisms of mucoadhesion. *Adv. Drug Delivery Rev.* **2005**, *57*, 1556–1568.
- (36) Cho, Y.; Kim, J. T.; Park, H. J. Size-controlled self-aggregated N-acetyl chitosan nanoparticles as a vitamin C carrier. *Carbohydr. Polym.* **2012**, *88*, 1087–1092.
- (37) Grant, J.; Blicher, M.; Piquette-Miller, M.; Allen, C. Hybrid films from blends of chitosan and egg phosphatidylcholine for localized delivery of Paclitaxel. *J. Pharm.* **2005**, *430*, 161–166.
- (38) Sonvico, F.; Cagnani, A.; Rossi, A.; Motta, S.; Di Bari, M. T.; Cavatorta, F.; Alonso, M. J.; Deriu, A.; Colombo, P. Formation of self-organized nanoparticles by lecithin/chitosan ionic interaction. *Int. J. Pharm.* **2006**, *324*, 67–73.